batteries

MDPI

*Review*

# Porous Electrode Materials for Zn-Ion Batteries: From Fabrication and Electrochemical Application

**Qixin Yang [1,2,†], Qingjiang Liu [2,†], Wei Ling [2], Haojiang Dai [1,2], Huanhui Chen [1,2], Jianghe Liu [2], Yejun Qiu [1,2] and Liubiao Zhong [1,2,*]**

[1] Shenzhen Engineering Lab of Flexible Transparent Conductive Films, Harbin Institute of Technology, Shenzhen 518055, China
[2] School of Materials Science and Engineering, Harbin Institute of Technology, Shenzhen 518055, China
* Correspondence: zhongliubiao@hit.edu.cn
† These authors contributed equally to this work.

**Abstract:** Porous materials as electrode materials have demonstrated numerous benefits for high-performance Zn-ion batteries in recent years. In brief, porous materials as positive electrodes provide distinctive features such as faster electron transport, shorter ion diffusion distance, and richer electroactive reaction sites, which improve the kinetics of positive electrode reactions and achieve higher rate capacity. On the other hand, the porous structures as negative electrodes also exhibit electrochemical properties possessing higher surface area and reducing local current density, which favors the uniform Zn deposition and restrains the dendrite formation. In view of their advantages, porous electrode materials for ZIB are expected to be extensively applied in electric and hybrid electric vehicles and portable electronic devices. In this review, we highlight the methods of synthesizing porous electrode materials and discuss the mechanism of action of porous structures as electrodes on their electrochemical properties. At the end of this review, the perspectives on the future development of porous materials in the field of electrochemical energy storage are also discussed.

**Keywords:** Zn-ion batteries; porous materials; fabrication; electrode; electrochemical application



**Citation:** Yang, Q.; Liu, Q.; Ling, W.; Dai, H.; Chen, H.; Liu, J.; Qiu, Y.; Zhong, L. Porous Electrode Materials for Zn-Ion Batteries: From Fabrication and Electrochemical Application. *Batteries* **2022**, *8*, 223. https://doi.org/10.3390/batteries8110223

Academic Editor: Guanjie He

Received: 29 September 2022
Accepted: 1 November 2022
Published: 7 November 2022



## 1. Introduction

Environment pollution and the energy crisis have emerged as two key issues owing to the wide application of fossil energy at present [1,2]. Developing new energy devices based on electrochemical energy storage plays a significant role in alleviating the sharply rising environmental pollution issue and promoting the sustainable development of human society [3,4]. Among them, lithium-ion batteries, dominating the market of rechargeable Metal-ion batteries, are extensively applied as an important power supply component for electronic devices in human life [1,5]. Although huge success has been achieved in the commercial field, the issues of safety, toxicity, high cost and the uneven distribution of lithium resources for LIBs still limit their development [6–8]. This is attributed to the fact that LIBs possess an unsafety liquid organic electrolyte [9]. Lithium batteries are very prone to explosion or fire when they are overcharged or continuously hot after a long time of use [10]. And lithium batteries generally use organic electrolyte in order to avoid contact with water and air, which not only increase the production cost and are apt to trigger fire and explosion in case of thermal runaway [11]. Therefore, people are actively looking for sustainable ways to produce new development chargeable batteries with safe and inexpensive to replace LIBs [12–14]. In contrast, zinc-ion batteries (ZIB) have natural advantages over lithium-ion batteries, including high safety and ionic conductivity (~1 S $cm^{-1}$ vs. 1 × $10^{-3}$ S $cm^{-1}$ for ZIB), ease of handling, and the ability to be assembled in atmospheric environment without glove box equipment [15–17]. Furthermore, ZIB also exhibits features of environment-friendly and inexpensive. These merits give the ZIB great promise for large-scale power grids [18–20].

As a predominant component of ZIBs, electrode materials have a key role in determining the electrochemical stability potential window and influencing the Coulombic efficiency of $Zn^{2+}$ storage and storage behavior. Among these electrode materials, porous materials have been widely concerned [21–24]. Generally speaking, the cathode materials of ZIB are mainly vanadium-based materials, manganese-based materials and Prussian blue. Prussian blue has a very high-voltage platform, but its capacity is too low. On the contrary, vanadium-based materials have a very low discharge platform despite their high specific capacity, which results in low power density and energy density of these two materials [25,26]. Compared with the other two materials, manganese-based materials have the moderate specific capacity and discharge platform advantages, but it is still difficult to show outstanding electrochemical performance [25,27]. Similarly, zinc anode materials are prone to produce zinc dendrites under non-uniform electric fields, leading to short circuits and battery failure. Therefore, in order to solve the disadvantages of low specific capacity and power density of energy storage devices and inhibit the growth of zinc anode dendrites, scientists focused on porous materials [10,28]. This is due to the fact that porous materials as positive/negative electrode materials possess significant advantages, such as (1) the pores structure of porous materials as electrode materials offer favorable access for the electrolyte to the electrode surface, (2) porous materials exhibit a relatively large surface area, which facilitates the transmission of charge at the electrode/electrolyte interface, (3) The active material wall around the pores is extremely thin, providing a short zinc ion diffusion length, (4) The porous structure boosts the electrocatalytic activity and stability of the electrode, due to the strengthened transportation of reactants to the nanoscale pore surface, (5) The porous structure uniformizes the local current density and electrical filed, stabilizing the zinc deposition [29–31].

Given these points, porous materials are among the most distinguished electrode materials, and they improve system performance very well while high current rates are required. In this review, we will discuss the preparation method to build porous positive/negative electrodes for ZIB. For example, common preparation methods for positive electrodes include soft templates and template-free methods. And effective fabrication approaches of negative electrodes contain hard templates, MOF templates and nice templates. Then, we will investigate the relationship between the porous structure of positive/negative electrodes and the electrochemical performance of ZIB by some examples. Finally, we will provide a brief outlook of the potential prospective applications of porous electrodes for the ZIB.

## 2. Fabrication of Porous Electrodes for ZIB

Porous materials are categorized according to their diameter of pores (micropores are 2 nm, mesopores are 2–50 nm, macropores are >50 nm), ordered or disordered morphology and methods of synthesis (template-based and non-template-based). The pore size and morphology of porous materials depend on their synthesis methods. In the following discussion, we first discuss that the synthesis method of porous materials has an effect on the size, structure and dimensions of the pores. Next, the effect of the porous materials as positive/negative electrodes on the electrochemical characteristics of ZIB was investigated [32].

### *2.1. Soft Templating of Porous Electrodes for ZIB*

In the synthesis of porous electrodes, soft templates (ST) with certain structural features have received great attention, which is formed by inter- and intra-molecular interactions (i.e., H-bonds, hydrophobic, hydrophilic interactions and electrostatic force) [33,34]. When using these STs, the pore shape and size of the PEM are adjustable by the selection of surfactant, solvent, and synthesis requirements, including nonordered mesopores and well-ordered mesopores featuring hexagonal, cubic, lamellar, or other symmetries [35,36]. ST is eliminated by extracting or calcining to yield porous electrode materials (PEMs). Commonly, STs like Pluronic P123 holds great promise for the construction of medium

manganese oxides and metals appropriate for ZIB as positive electrode and are not widely employed in negative electrodes. Therefore, we concentrate solely on the application of ST in the positive electrode for ZIB.

Porous Materials as Positive Electrode Made by Soft Templates for ZIB

Feng D et al. [37] reported that the high rate ZIB performance was achieved by the rational design of $Mn_2O_3$ Mesoporous structured cathodes, as shown in Figure 1a,b. $Mn_2O_3$, as a positive electrode with interconnected porous structures and adjustable porosity size, was synthesized utilizing Pluronic P123 as a soft template. Due to the presentation of nanoporous architecture, the prepared ZIB devices demonstrated remarkably improved rate capability and outstanding cycling durability.

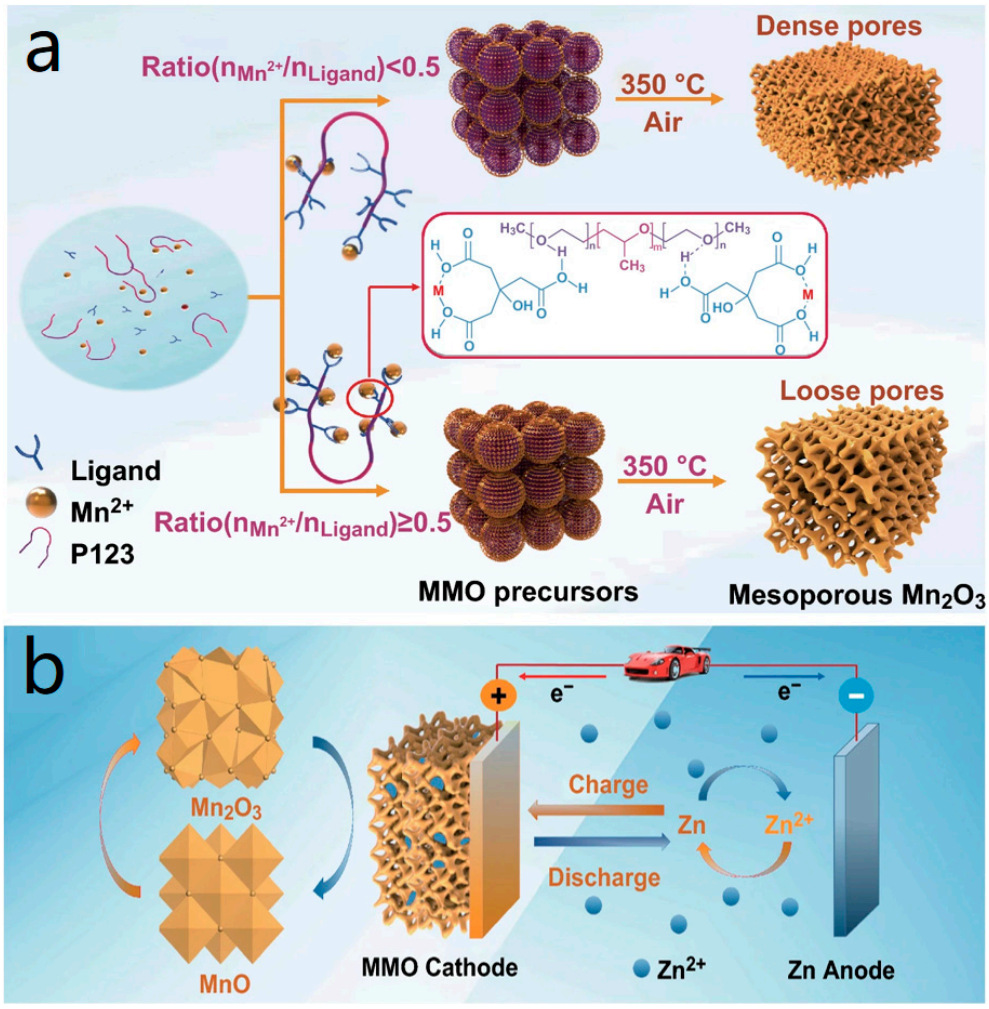


**Figure 1.** (**a**) Schematic illustration of the preparation process of $Mn_2O_3$ Mesoporous structured cathodes. (**b**) Schematic Illustration of charge/discharge process of Zn||$Mn_2O_3$ aqueous rechargeable battery. Reproduced with permission from reference [27].

Although the flexible film plate method provides considerable advantages in constructing porous structures of positive electrode materials, however, it is difficult to extend to the construction of a broad range of porous positive electrode materials. Therefore, the present review only mentioned it and did not elaborate too much.

### *2.2. Hard Templating of Porous Electrodes for ZIB*

During the fabrication of PEM featuring variable components and morphologies, ST was a powerful method. Yet, it is very difficult sometimes that ordered PEMs, having a high

degree of crystalline walls, to be obtained; this is due to the fact that the inorganic phase crystallizes at a temperature higher than the temperature of ST removal [38]. More often, the absence of supporting surfactants from the assembly and the crystallites sintering will cause a broken ring in the porous structure. In contrast to soft templates, hard templates (HTs) have received widespread attention because their rigid structure is not altered by interacting with precursors. When a hard template is used, inorganic precursors enter the pores or pore walls of the hard template by immersion, electrodeposition and other methods. Subsequently, the hard template is removed by high temperature, organic solutions, etc., yielding a porous structure with an inorganic framework. Among HTs, Inverse opal (IO) structures, including assemblies of colloidal particles and top-down lithography-based technologies, have been extensively utilized as positive/negative electrodes for ZIBs due to porous electrodes with well-ordered [39].

Allowing kinds of preparing methods of IO structure, colloidal crystal templating (CCT) has been received attention due to relatively simple and inexpensive [40–42]. During this methodology, mono-dispersed polymer spheres (PS, PMMA) or silicon spheres have been assembled into periodic arrays under the action of hydrogen bonding, capillary attraction, shear force and gravity. The targeted PEM precursor solution has been injected into the void between the spheres. Thermal processing then transforms the precursor into a skeleton of solids that surrounds the template sphere. Finally, in order to remove the polymer or silica template to obtain the IO structure, two methods can be used: (1) The removal of polymer sphere templates, such as PS or PMMA spheres, was also accomplished by calcination in the air above 350 °C. (2) The silicon sphere would be removed by etching, for example, employing a hydrofluoric acid solution. Based on the above methods, the prepared IO structures as PEM exhibit two characteristics. One is that the pore size can be adjusted by resizing the colloidal polymer or silica spheres to variable the pore size. Secondly, the wall morphology, the degree of crystallinity and the skin texture could be controlled by altering the removal requirement of the template. The following section reviews the application of inverse opal (IO) structures of materials as positive/negative electrodes in the construction of ZIBs for the fabrication of porous electrodes.

#### 2.2.1. Inverse Opal (IO) Structures of Materials as Positive Electrode for ZIB

By using excellent features of IO structures as positive electrodes, efforts have been made to explore various interesting ZIBs with superior electrochemical performance for years. For example, H Ren et al. [29] reported the synthesis of $MnO_2$ with IO structure as a positive electrode using PS as a template by solution method. This IO structure allows effective separation of nanosheets in the presence of aggregation, forming several layers of $MnO_2 \cdot 0.44\ H_2O$ and even ultrathin nanosheets having thicknesses down to 1 nm. In addition, Zinc-ion aqueous batteries constructed from the IO structure of manganese dioxide have excellent properties, which include a very high-level comparative discharge capacity of up to 300 mA $g^{-1}$ current density, maintaining a high-power discharge capacity of 262.9 mAh $g^{-1}$ over 100 cycles, and even achieving a higher current density of 2000 mA $g^{-1}$ after 5000 cycles at 121 mAh $g^{-1}$ high power discharge capacity.

Based on the above discussion, the IO structure as the positive electrodes has the potential of separating the nanosheets effectively in the presence of nanosheet aggregation, increasing and expanding the interlayer space of positive electrode nanosheets, which further ensures excellent high-rate performance [6].

#### 2.2.2. Inverse Opal (IO) Structures of Materials as Negative Electrode for ZIB

Moreover, the IO structures as negative electrode guests uniformize local current density and electrical field and stabilize zinc deposition. PX Sun et al. [38] have developed a TZNC IO mainframe that modulates the deposition of zinc by CCT (use of PS spheres as templates) and through topochemical reactions (Figure 2a–d). It is worth noting that the 3D microporous framework with IO structure can inhibit the growth of Zn dendrites. In addition, TZNC IO has adequate voids to provide effective adjustments of zinc ion fluxes

and to relieve volume expansion Thanks to spatial tuning and optimized combination; the TZNC IO host can achieve uniform Zn deposition at lower nucleation potentials with a lifetime of more than 450 h (Figure 2b). Moreover, the water-based ZIB, which is assembled from a TZNC@Zn anode and the commercial $V_2O_5$ cathode, shows exceptional reversible properties and favorable cycling stability of over 2000 cycles (Figure 2c,d).

Apart from CCT, top-down lithography-based technologies (LT) also is a good method for preparing IO structure as prepared IO structure has a damage-free structure and a controllable structure with a through-hole structure. In this method, the metal element is deposited in the void of the conductive opal structure by way of electrodeposition, which is prepared by LT [43,44]. Finally, in order to obtain an electrode material with an IO metal structure, the opal structure can be removed by an organic solution [26]. Concerning these advantages, a number of higher performances of ZIBs were developed. Liu H et al. [45] reported the fabrication of ZIB having high specific energy through a combination of photolithography and electrochemical processing techniques (Figure 2e,f). Compared with most investigated structurally engineered Zn anodes, the IO structures prepared by LT accurately governed the actual dimension of the 3D network and efficiently tuned the micro/nanostructures, taking full advantage of the 3D structures. And the unique microporous engineered Zn-based IO structures displayed favorable flexibility and improved mechanical strength. In addition, the Zn-based IO structures have a lower overpotential and higher cyclic stability than the planar Zn films. Importantly, it is notable that the collector-free ultralight Zn microgrids have great potential in high-specificity energy batteries.

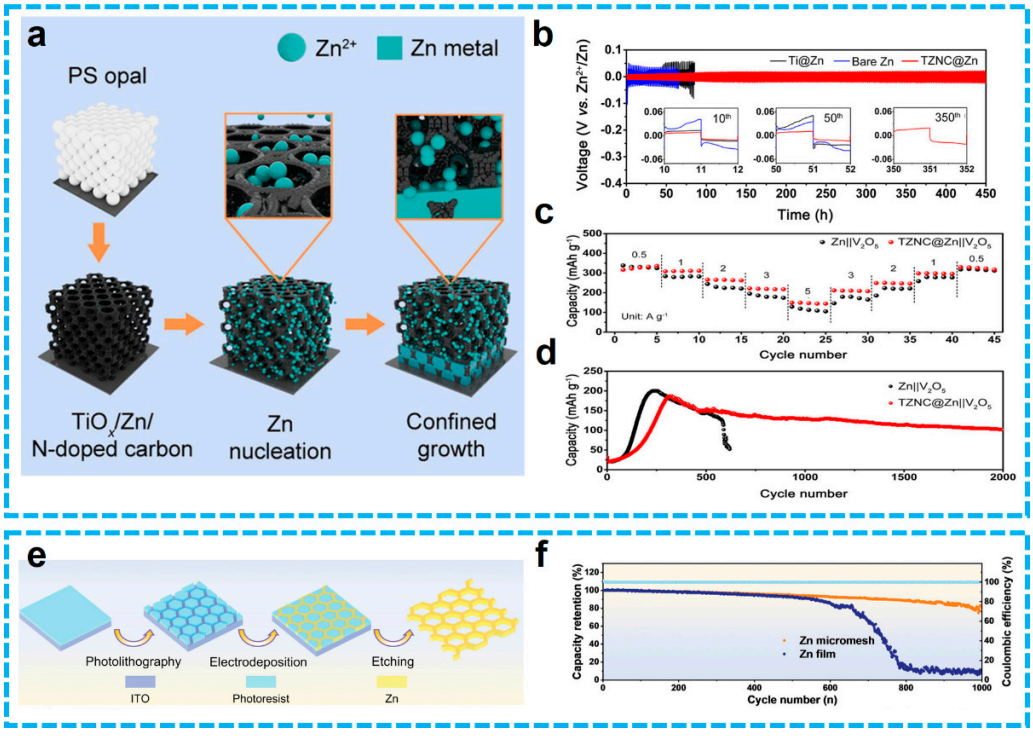


**Figure 2.** (**a**) Schematic illustration of the procedure for the TZNC IO and Zn deposition on the TZNC host Reproduced with permission from reference [31]. (**b**) Voltage profiles of Zn plating/stripping in symmetric batteries with a capacity of 1 mAh $cm^{-2}$ at 1 mA $cm^{-2}$ Reproduced with permission from reference [31]. (**c**) Rate performances and (**d**) cycling performance at 5 A $g^{-1}$ for TZNC@Zn | | $V_2O_5$ and Zn | | $V_2O_5$ full cells Reproduced with permission from reference [38]. (**e**) Schematic illustration of the fabrication process of Zn-based IO structure Reproduced with permission from reference [32]. Reproduced with permission from reference. (**f**) Long-term cycling test of ZM//PVO and ZF//PVO pouch batteries at the current density of 10 A $g^{-1}$ Reproduced with permission from reference [45].

In view, the negative electrode exhibits IO structures, prepared by assemblies of colloidal particles and top-down lithography-based technologies, which can boast a greater surface area and lower local current density, which facilitates homogeneous zinc deposition and the formation of restrained dendrites.

### *2.3. Metal-Organic Framework (MOF) Derived Porous Electrodes for ZIB*

As an alternative to synthetic templates, MOF-derived porous materials as ideal electrodes for ZIB, exhibiting the advantages of controllable porous structures without the need for additional templates or cumbersome procedures, have been investigated in recent years. This is owing to their persistent inherent porosity and metal species [43,46]. As organic-inorganic hybrid materials with intramolecular pores, MOFs consist of the self-assembly of organic ligands and coordination bonds of metal ions or clusters [47]. In the preparation process, the use of suitable manipulation approaches is crucial for the conversion of MOF precursors into functionally derived compounds. They are due to that these techniques significantly affect the micro/nanostructure and composition of the end products. Depending on the reaction mechanism, the subsequent conversion methodology is divided into the following four categories: (a) self-pyrolysis in an inert/air environment, (b) chemical reactions with relevant gas/vapor ligands, (c) chemical reactions with liquid ligands, and (d) chemical reactions with a solid ligand. However, the porous electrodes based on MOF prepared by the second method are rarely used in ZIB. Here, this following discussion highlights three methods except the second method on the fabrication of MOFs and the investigation of their derived porous positive electrode on the electrochemical performance of ZIB.

#### 2.3.1. Porous Materials as Negative Electrode Made by MOF for ZIB

Self-pyrolysis template technique is an active technique for the construction of porous materials derived from MOFs under inert/air conditions. In this process, MOFs with good confinement may be created by using raw materials as templates and sacrificing them throughout the development process. The obtained MOFs exhibit some advantages providing suitable building blocks after calcination, heterojunction structure, high porosity and different dimensions. They can further boost the electrical conductivity and enhance the active sites as well as preserve their advantages, which lead to rapid mass/charge transfer and strengthened electrochemical properties. Of great importance is that MOF-based anodes have shown great efficiency during zinc plate stripping and have protected against the formation of dendrites. For example, Yuksel R et al. [48] have reported designing and constructing novel MOF-based zinc anodes for dendritic-free, higher-performance ZIBs. As shown in Figure 3a,b, the intimate contact between the zinc anode and the electrolyte prevents any gaps or spaces from forming, which prevents dendrite formation and permits a single type of charge distribution during the zinc plating-stripping process. Ions can move through the top layer during cycling, but dendrite development in the pores of the redesigned zinc anode surface is almost impossible. Based on these excellent properties, the manufactured ZIBs have an extremely long cycle life.

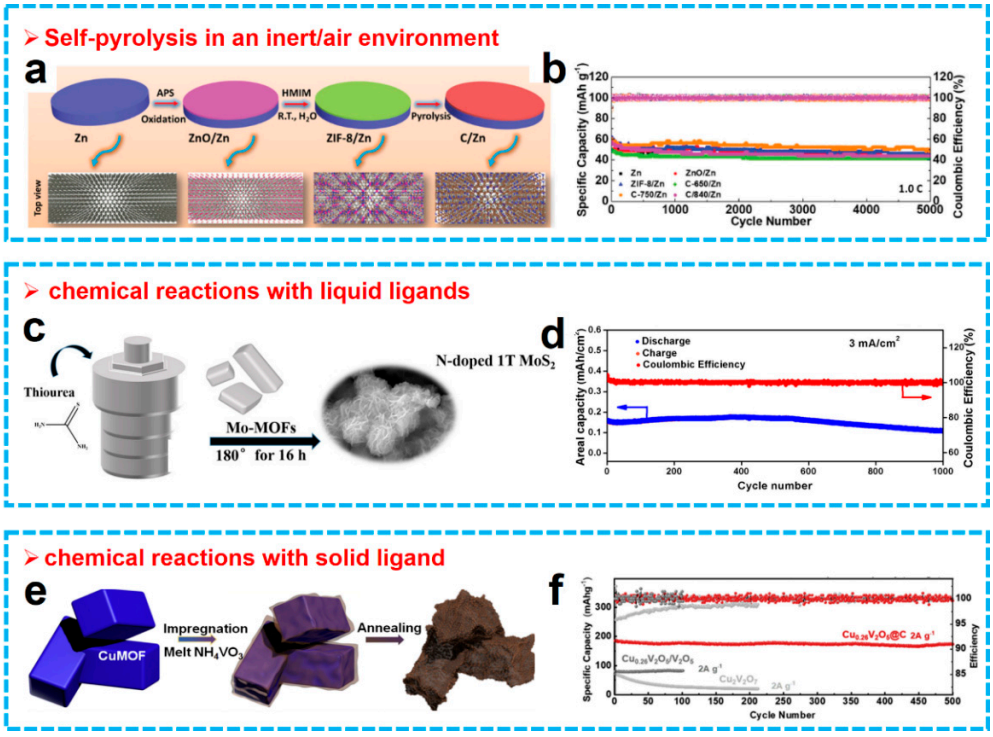


**Figure 3.** (**a**) Schematic of the fabrication process and the predicted top and side views of the Zn anode. (**b**) Cycling performance of the ZIB at 1.0 C Reproduced with permission from reference [48]. (**c**) Illustration of the preparation process of N-Doped 1T $MoS_2$. (**d**) Long-term cycle performance at 3 mA $cm^{-2}$ with mass loading of 1.897 mg $cm^{-2}$ Reproduced with permission from reference [49]. (**e**) The schematic diagram of the melt-infiltration fabrication strategy for $Cu_{0.26}V_2O_5$@C. (**f**) the cycling performance under 2 A $g^{-1}$ Reproduced with permission from reference.

#### 2.3.2. Porous Materials as Positive Electrode Made by MOF for ZIB

One of the most promising materials for ZIB is MOF-derived homogeneous heteromaterials, which are produced by the reaction of liquid organic ligands with metal ions from MOF templates/precursors [50]. In particular, the production of MOF derivatives with manageability is more feasible due to the orientation guidance of the MOF precursor/template and the high fluidity of the variable liquid organic ligands in solution or molten state. Production of MOF derivatives with manageability is a more feasible structure and composition [51]. For example, Sheng Z et al. [49] create N-doped 1T $MoS_2$ porous nanoflowers by hydrothermally sulfurizing the Mo-MOF used as the nitrogen supply in a single step (Figure 3c,d). The performance of N-doped 1T $MoS_2$ porous nanoflowers is better than that of pure porous 1 T $MoS_2$ and 2 H $MoS_2$ made by using molybdenum source $MoO_3$. After 1000 cycles, ZIB maintained 89.1% of its capacity at 3000 mA $g^{-1}$ as provided, demonstrating high cycling stability.

Another efficient technique for the synthesis of MOF-derived functional materials is the interfacial coordination reaction between solid organic ligands and MOF precursors/templates without the use of solvents [52]. This procedure involves the release of metal ions from MOF templates or precursors, which are then used to form homogeneous mixtures through a precise coordination reaction with solid organic ligands. Similar to how old bonds in mixtures break and new forms in metal-based precursors, this reaction is accompanied by both. For example, Wang X et al. [53] illustrated how straight conversion and impregnation of Cu-doped $V_2O_5$ with layered porous carbon composite ($Cu_{0.26}V_2O_5$@C) was used as a cathode for ZIB (Figure 3e,f). The hierarchical pores in this protocol can be used to boost contact of the dynamic material with the electrolyte and attain the electrolyte's effectual penetration into the material, whereas the carbon host can make the electronic conductivity easier. Cu doping can advance zinc ions' immigration

by widening and balancing $V_2O_5$'s layered structure. The prepared ZIB exhibits brilliant electrochemical properties, which include as an effect of extremely precise capacity combination (328.8 mAh $g^{-1}$ at 200 mA $g^{-1}$), favorable rate performance (163.8 mAh $g^{-1}$ at 2000 mA $g^{-1}$), and noteworthy cycling stability (93.5% capability retention after 500 cycles).

### *2.4. Ice Templating Porous Materials for ZIB*

As a non-polluting and sustainable template, ice templates, also known as cryocasting, are a particularly universal technology that has been widely used to fabricate controllable bionanoporous materials based on metals, polymers, biomolecules and carbon nanomaterials, endowing them with new characteristics and expanding their range of applications [54–57] (Figure 4). In this process, the ice templating method can be divided into three steps: (1) The preparation of frozen precursors such as solutions, suspensions or gels, providing the fundamental basis for obtaining ideal three-dimensional structures, (2) the controlled solidification (freezing) of the above-mentioned precursors such as solutions, suspensions or gels, (3) Solvents (usually water) under reduced pressure sublimation, (4) other subsequent treatments.

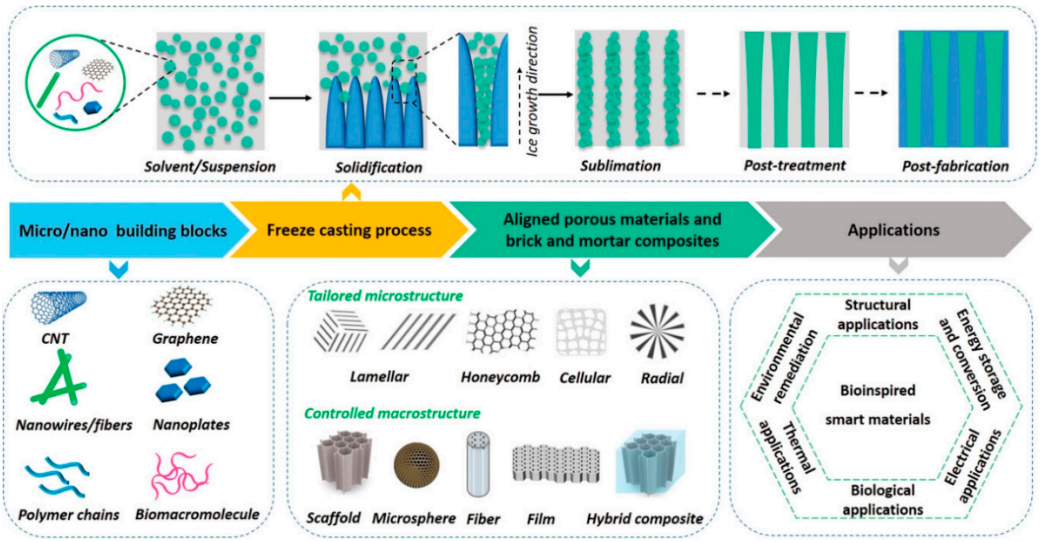


**Figure 4.** Schematic diagram of the themes discussed in this review, from the macroscopic assembly of micro/nano building blocks to emerging applications, Reproduced with permission from reference [42].

When constructing three-dimensional porous materials by the ice template method, the regulation of the solvent solidification (freezing) process is the key to the modification of the microstructure of the materials to produce materials with different properties. For example, the pore size of the materials and their morphology is determined by the temperature, speed and other factors during the freezing process [58–60]. Based on the advantage of these features, ice-templated derived porous materials as negative electrodes for ZIB have been discussed in the following review.

#### Porous Materials as Negative Electrode Made by Ice Templating for ZIB

For example, Zhou J et al. [61] have invented a three-dimensional elastic MXene/graphene scaffold through a directed freezing procedure. Owing to the microporosity and plentiful zinc-loving characteristics in the structure, zinc is densely implanted in the host throughout the electrodeposition method. Over cycling, the composite anode imparts an in situ solid electrolyte interface of fluorinated zinc at the electrode/electrolyte interface thanks to the intrinsic fluorine termination in MXene, which restrains dendritic growth effectively. Hence, the electrode achieved a prolonged cycle life of more than 1000 h at 10 mA $cm^{-2}$ in symmetric ZIB tests. Ling W et al. [62] have reported a three-dimensional

lightweight silver nanowire aerogel (AgNWA) through a directed freezing process to direct a homogeneous Zn plating/stripping process within confined conditions. Compared to the planar structure of the electrode, the three-dimensional cross-linked fiber structure provides a uniformly distributed electric field for homogeneous Zn deposition/exfoliation.

Ice-templated porous negative materials not only efficiently introduce the consistent nucleation of Zn but likewise provide foldable strength for an elastic 3D host to construct corresponding wearable energy storage systems.

### *2.5. Non-Templated Porous Materials for ZIB*

This review's principal focal point has been porous ZIB materials that possess structure or favorable pore size, and this is considerably accessed by applying templating approaches. However, there are also many template-free methods to fabricate porous electrodes, which include ultrasonic methods [63–65], intercalation [66,67], electrodeposition [39,68,69], aqueous or solvothermal synthesis [70,71] and others. While these techniques have the inclination to produce materials that exhibit a wider pore size distribution, several of these approaches furnish more fantastic simplicity than those that require templates, and materials of crucial and distinctive dimensions facilitating electrode characteristics can be produced. However, here we only discuss hydrothermal synthesis as a method and the effect of the porous materials as a positive electrode on the electrochemical properties of ZIB [47].

#### Porous Materials as Positive Electrode Made by Non-Templated for ZIB

Solvothermal syntheses are well suited to produce PEM. For example, Chen L et al. [71] reported that hollow $V_2O_5$ nanospheres that had a shell thickness of 50 nm and a diameter of approximately 450 nm were synthesized through a template-free solvothermal technique in combination with the calcination remedy (Figure 5a,b). This nano-sized hollow structure can control the volume expansion under the charging/discharging process, which gives it excellent cycling stability. At the same time, the majority of hollow structures can maintain their pristine structure during long-term cycling. Besides, the excellent surface area's presence makes hollow structures dominate impenetrable electrochemically active sites, where the unusual effectual contact region between electrode and electrolyte permits expeditious diffusion of electrons and ions. Ameliorated electrochemical performance is promoted by these unusual properties of the nanoscale hollow structure, including more unusual cycling stability and rate capability, reaching 147 mAh $g^{-1}$ after 6000 cycles at 10 A $g^{-1}$ and an outstanding reversible capacity of 327 mAh $g^{-1}$ at 100 mA $g^{-1}$. Yet at 15 A $g^{-1}$, the specific capacity can still reach 122 mAh $g^{-1}$ after 10,000 cycles. Moreover, Hu P et al. [72] synthesized an anhydrous $V_2O_5$ yolk-shell cathode ($V_2O_5$-YS) with high performance by an uncomplicated template-free solvothermal procedure (Figure 5c). By reason of the porous yolk-shell structure, the $V_2O_5$-YS could advance rapid electrolyte transport for the most part and, in a similar way, keep structural collapse over cycling. In consequence, 410 mA h $g^{-1}$'s brilliant reversible capacities are exhibited by prepared ZIB at 100 mA $g^{-1}$ and 182 mA h $g^{-1}$ at 20 A $g^{-1}$, and a capacity retention of 80% is obtainable above 1000 cycles at 5.0 A $g^{-1}$ (Figure 5d).

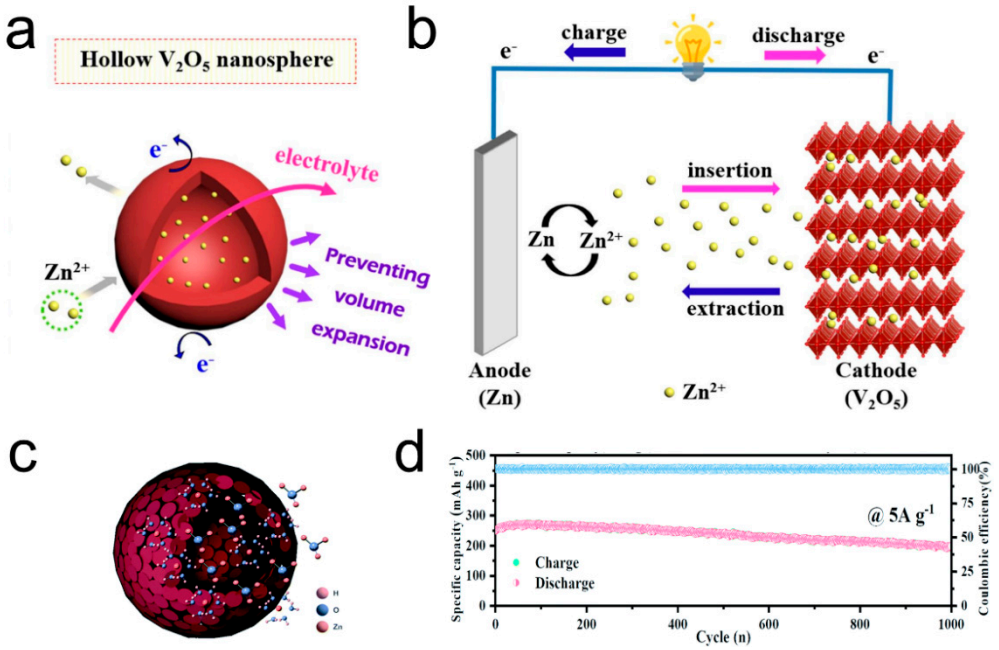


**Figure 5.** (**a**,**b**) The fabrication of Hollow $V_2O_5$ nanospheres and their electrochemical properties Reproduced with permission from reference [60]. (**c**,**d**) Schematic of the as-prepared $V_2O_5$−YS microspheres and their electrochemical properties Reproduced with permission from reference [61].

## 3. Conclusions and Perspective

These positive/negative electrodes can provide excellent zinc flux throughout the interface, brief diffusion pathways for zinc insertion/extraction and electrons, extra dynamic sites at the electrolyte-electrode interface, and freedom for volume expansion/contraction throughout charge/discharge cycles. In this review, porous motor materials preparation by the template approach is summarized, and pore size's influence and morphology of porous materials on ZIBs' electrochemical characteristics are similar way concisely touched upon. It, nevertheless, is not explicit morphology or which pore size accomplishes the most excellent performance. In addition to soft templating, hard templating, metal-organic framework, ice templating and non-templated, vacuum deposition technologies, such as Chemical Vapor Deposition (CVD), Atomic layer deposition (ALD), and Physical Vapor Deposition (PVD) can also be used for the preparation of porous materials, which have great application prospects in the field of energy storage. In the future, the more necessary study is consequently wanted to complete organic compatibility between the electrochemical performance and porous structure of the material and to accomplish the most wonderful electrochemical performance. (1) experimental and theoretical studies to correlate the dependence of porosity, morphology and pore size on cycling performance (2) should improve Coulombic efficiency by optimizing SEI's formation on porous structures (3) volume capacity needs to be attached importance, which is a vital parameter for high power applications, and (4) simple, scalable and low-cost fabrication processes need be developed.

Although porous materials have gained great application space in the field of energy storage, there is still a long way to go before they can be industrialized. This is not only because the relationship and mechanism between porous materials and outstanding electrochemical properties have not been fully studied but also because the development of porous materials requires relatively high costs. Porous materials can endow electrode materials with higher specific surface area and increase reaction sites, but their synthesis steps are very complex, and it is difficult to produce and prepare them on a large scale. At the same time, their morphology observation and characterization schemes are expensive, so they are still mainly in the laboratory synthesis and testing stage. Not only that, up to now, there are few actual cases of directly using porous materials in the industrial and

commercial energy storage field. Therefore, we should speed up the batch preparation of porous materials, reduce the preparation cost, and optimize the preparation process and flow so as to accelerate the industrialization process of porous materials.

**Author Contributions:** Q.Y. and Q.L. contributed equally to searching the literature and drafted the majority of this paper. W.L., H.D., H.C. and J.L. contributed to the manuscript design and refinement. L.Z. and Y.Q. revised the paper and conducted the literature-screening efforts. All authors have read and agreed to the published version of the manuscript.

**Funding:** The authors gratefully acknowledge the financial support by Shenzhen Municipality under the Project of the National Natural Science Foundation of China (No. 51971080), the Fundamental Research Funds for the Central Universities (Grant No. HIT.OCEF.2021034), and Shenzhen Bureau of Science, Technology and Innovation Commission (GXWD20201230155427003-20200730151200003 and JSGG20200914113601003).

**Data Availability Statement:** Not applicable.

**Conflicts of Interest:** The authors declare no conflict of interest.

## References

1. Mo, F.; Guo, B.; Liu, Q.; Ling, W.; Liang, G.; Chen, L.; Yu, S.; Wei, J. Additive manufacturing for advanced rechargeable lithium batteries: A mini review. *Front. Energy Res.* **2022**, *10*, 986985. [CrossRef]
2. Hussain, I.; Lamiel, C.; Sahoo, S.; Ahmad, M.; Chen, X.; Javed, M.S.; Qin, N.; Gu, S.; Li, Y.; Nawaz, T.; et al. Factors affecting the growth formation of nanostructures and their impact on electrode materials: A systematic review. *Mater. Today Phys.* **2022**, *27*, 100844. [CrossRef]
3. Li, Y.; Wu, Y.; Ma, T.; Wang, Z.; Gao, Q.; Xu, J.; Chen, L.; Li, H.; Wu, F. Long-Life Sulfide All-Solid-State Battery Enabled by Substrate-Modulated Dry-Process Binder. *Adv. Energy Mater.* **2022**, *12*, 2201732. [CrossRef]
4. Xie, C.; Yan, D.; Li, H.; Du, S.; Chen, W.; Wang, Y.; Zou, Y.; Chen, R.; Wang, S. Defect chemistry in heterogeneous catalysis: Recognition, understanding and utilization. *Acs Catal.* **2020**, *10*, 11082–11098. [CrossRef]
5. Liu, Q.; Ji, Z.; Mo, F.; Ling, W.; Wang, J.; Lei, H.; Cui, M.; Zhang, Z.; Liu, Y.; Cheng, L.; et al. Stable Thermochromic Hydrogel for a Flexible and Wearable Zinc-Ion Yarn Battery with High-Temperature Warning Function. *ACS Appl. Energy Mater.* **2022**, *5*, 12448–12455. [CrossRef]
6. Schmidt, O.; Hawkes, A.; Gambhir, A.; Staffell, I. The future cost of electrical energy storage based on experience rates. *Nat. Energy* **2017**, *2*, 17110. [CrossRef]
7. Liu, J.; Ahmed, S.; Wang, T.; Song, S. Flexible thermotolerant Zn-ion hybrid supercapacitors enabled by heat-resistant polymer electrolyte. *Chem. Eng. J.* **2023**, *451*, 138512. [CrossRef]
8. Yang, S.; Zhang, F.; Ding, H.; He, P.; Zhou, H. Lithium metal extraction from seawater. *Joule* **2018**, *2*, 1648–1651. [CrossRef]
9. Liu, Y.; Li, W.; Cheng, L.; Liu, Q.; Wei, J.; Huang, Y. Anti-Freezing Strategies of Electrolyte and their Application in Electrochemical Energy Devices. *Chemal Rec.* **2022**, *22*, e202200068. [CrossRef]
10. Mu, Y.; Han, M.; Wu, B.; Wang, Y.; Li, Z.; Li, J.; Li, Z.; Wang, S.; Wan, J.; Zeng, L. Nitrogen, Oxygen-Codoped Vertical Graphene Arrays Coated 3D Flexible Carbon Nanofibers with High Silicon Content as an Ultrastable Anode for Superior Lithium Storage. *Adv. Sci.* **2022**, *9*, e2104685. [CrossRef]
11. Mackanic, D.G.; Chang, T.-H.; Huang, Z.; Cui, Y.; Bao, Z. Stretchable electrochemical energy storage devices. *Chem. Soc. Rev.* **2020**, *49*, 4466–4495. [CrossRef] [PubMed]
12. Liu, Q.; Chen, R.; Xu, L.; Liu, Y.; Dai, Y.; Huang, M.; Mai, L. Steric Molecular Combing Effect Enables Ultrafast Self-Healing Electrolyte in Quasi-Solid-State Zinc-Ion Batteries. *ACS Energy Lett.* **2022**, *7*, 2825–2832. [CrossRef]
13. Liu, J.; Khanam, Z.; Ahmed, S.; Wang, T.; Wang, H.; Song, S. Flexible antifreeze zn-ion hybrid supercapacitor based on gel electrolyte with graphene electrodes. *ACS Appl. Mater. Interfaces* **2021**, *13*, 16454–16468. [CrossRef] [PubMed]
14. Kundu, D.; Adams, B.D.; Duffort, V.; Vajargah, S.H.; Nazar, L.F. A high-capacity and long-life aqueous rechargeable zinc battery using a metal oxide intercalation cathode. *Nat. Energy* **2016**, *1*, 16119. [CrossRef]
15. Dong, H.; Li, J.; Guo, J.; Lai, F.; Zhao, F.; Jiao, Y.; Brett, D.J.; Liu, T.; He, G.; Parkin, I.P. Insights on flexible zinc-ion batteries from lab research to commercialization. *Adv. Mater.* **2021**, *33*, 2007548. [CrossRef]
16. Lv, Y.; Xiao, Y.; Ma, L.; Zhi, C.; Chen, S. Recent Advances in Electrolytes for "Beyond Aqueous" Zinc-Ion Batteries. *Adv. Mater.* **2022**, *34*, 2106409. [CrossRef]
17. Zhu, Y.; Yin, J.; Zheng, X.; Emwas, A.-H.; Lei, Y.; Mohammed, O.F.; Cui, Y.; Alshareef, H.N. Concentrated dual-cation electrolyte strategy for aqueous zinc-ion batteries. *Energy Environ. Sci.* **2021**, *14*, 4463–4473. [CrossRef]
18. Fang, G.; Zhou, J.; Pan, A.; Liang, S. Recent advances in aqueous zinc-ion batteries. *ACS Energy Lett.* **2018**, *3*, 2480–2501. [CrossRef]
19. Blanc, L.E.; Kundu, D.; Nazar, L.F. Scientific challenges for the implementation of Zn-ion batteries. *Joule* **2020**, *4*, 771–799. [CrossRef]

20. Liu, C.; Xie, X.; Lu, B.; Zhou, J.; Liang, S. Electrolyte strategies toward better zinc-ion batteries. *ACS Energy Lett.* **2021**, *6*, 1015–1033. [CrossRef]
21. Ma, H.; Tian, X.; Wang, T.; Tang, K.; Liu, Z.; Hou, S.; Jin, H.; Cao, G. Tailoring Pore Structures of 3D Printed Cellular High-Loading Cathodes for Advanced Rechargeable Zinc-Ion Batteries. *Small* **2021**, *17*, 2100746. [CrossRef] [PubMed]
22. Liu, P.; Gao, Y.; Tan, Y.; Liu, W.; Huang, Y.; Yan, J.; Liu, K. Rational design of nitrogen doped hierarchical porous carbon for optimized zinc-ion hybrid supercapacitors. *Nano Res.* **2019**, *12*, 2835–2841. [CrossRef]
23. Wang, J.; Liu, Z.; Wang, H.-g.; Cui, F.; Zhu, G. Integrated pyrazine-based porous aromatic frameworks/carbon nanotube composite as cathode materials for aqueous zinc ion batteries. *Chem. Eng. J.* **2022**, *450*, 138051. [CrossRef]
24. Fu, Y.; Wei, Q.; Zhang, G.; Wang, X.; Zhang, J.; Hu, Y.; Wang, D.; Zuin, L.; Zhou, T.; Wu, Y. High-Performance Reversible Aqueous Zn-Ion Battery Based on Porous MnOx Nanorods Coated by MOF-Derived N-Doped Carbon. *Adv. Energy Mater.* **2018**, *8*, 1801445. [CrossRef]
25. Hussain, I.; Ahmad, M.; Chen, X.; Abbas, N.; Al Arni, S.; Salih, A.A.M.; Benaissa, M.; Ashraf, M.; Ayaz, M.; Imran, M.; et al. Glycol-assisted Cu-doped ZnS polyhedron-like structure as binder-free novel electrode materials. *J. Saudi Chem. Soc.* **2022**, *26*, 101510. [CrossRef]
26. Wu, B.; Mu, Y.; Li, Z.; Li, M.; Zeng, L.; Zhao, T. Realizing high-voltage aqueous zinc-ion batteries with expanded electrolyte electrochemical stability window. *Chin. Chem. Lett.* **2022**. [CrossRef]
27. Liu, Q.; Yang, L.; Ling, W.; Guo, B.; Chen, L.; Wang, J.; Zhang, J.; Wang, W.; Mo, F. Organic electrochromic energy storage materials and device design. *Front. Chem.* **2022**, *10*, 1001425. [CrossRef]
28. Yang, L.; Liu, Q.; Liu, Y.; Chen, X.; Luo, J.; Huang, Y. Shape-Memory Electrochemical Energy Storage Devices. *Batter. Supercaps* **2022**, *5*, 202200275. [CrossRef]
29. Ren, H.; Zhao, J.; Yang, L.; Liang, Q.; Madhavi, S.; Yan, Q. Inverse opal manganese dioxide constructed by few-layered ultrathin nanosheets as high-performance cathodes for aqueous zinc-ion batteries. *Nano Res.* **2019**, *12*, 1347–1353. [CrossRef]
30. Ding, Y.; Peng, Y.; Chen, S.; Zhang, X.; Li, Z.; Zhu, L.; Mo, L.-E.; Hu, L. Hierarchical porous metallic $V_2O_3$@ C for advanced aqueous zinc-ion batteries. *ACS Appl. Mater. Interfaces* **2019**, *11*, 44109–44117. [CrossRef]
31. Tang, K.; Yuan, C.; Xiong, Y.; Hu, H.; Wu, M. Inverse-opal-structured hybrids of N, S-codoped-carbon-confined $Co_9S_8$ nanoparticles as bifunctional oxygen electrocatalyst for on-chip all-solid-state rechargeable Zn-air batteries. *Appl. Catal. B Environ.* **2020**, *260*, 118209. [CrossRef]
32. Zhou, J.; Zhang, R.; Xu, R.; Li, Y.; Tian, W.; Gao, M.; Wang, M.; Li, D.; Liang, X.; Xie, L. Super-Assembled Hierarchical Cellulose Aerogel-Gelatin Solid Electrolyte for Implantable and Biodegradable Zinc Ion Battery. *Adv. Funct. Mater.* **2022**, *32*, 2111406. [CrossRef]
33. Lu, Y. Surfactant-Templated Mesoporous Materials: From Inorganic to Hybrid to Organic. *Angew. Chem. Int. Ed.* **2006**, *45*, 7664–7667. [CrossRef] [PubMed]
34. Lee, A.F.; Bennett, J.A.; Manayil, J.C.; Wilson, K. Heterogeneous catalysis for sustainable biodiesel production via esterification and transesterification. *Chem. Soc. Rev.* **2014**, *43*, 7887–7916. [CrossRef]
35. Wang, H.; Shao, Y.; Mei, S.; Lu, Y.; Zhang, M.; Sun, J.-K.; Matyjaszewski, K.; Antonietti, M.; Yuan, J. Polymer-derived heteroatom-doped porous carbon materials. *Chem. Rev.* **2020**, *120*, 9363–9419. [CrossRef] [PubMed]
36. Xie, Y.; Kocaefe, D.; Chen, C.; Kocaefe, Y. Review of research on template methods in preparation of nanomaterials. *J. Nanomater.* **2016**, *2016*, 2302595. [CrossRef]
37. Feng, D.; Gao, T.-N.; Zhang, L.; Guo, B.; Song, S.; Qiao, Z.-A.; Dai, S. Boosting high-rate zinc-storage performance by the rational design of $Mn_2O_3$ nanoporous architecture cathode. *Nano-Micro Lett.* **2020**, *12*, 14. [CrossRef]
38. Sun, P.X.; Cao, Z.; Zeng, Y.X.; Xie, W.W.; Li, N.W.; Luan, D.; Yang, S.; Yu, L.; Lou, X.W. Formation of Super-Assembled $TiO_x$/Zn/N-Doped Carbon Inverse Opal Towards Dendrite-Free Zn Anodes. *Angew. Chem. Int. Ed.* **2022**, *61*, e202115649.
39. Wang, M.; Zhang, F.; Lee, C.S.; Tang, Y. Low-cost metallic anode materials for high performance rechargeable batteries. *Adv. Energy Mater.* **2017**, *7*, 1700536. [CrossRef]
40. Yeo, S.J.; Choi, G.H.; Yoo, P.J. Multiscale-architectured functional membranes utilizing inverse opal structures. *J. Mater. Chem. A* **2017**, *5*, 17111–17134. [CrossRef]
41. Hsieh, C.-H.; Lu, Y.-C.; Yang, H. Self-assembled mechanochromic shape memory photonic crystals by doctor blade coating. *ACS Appl. Mater. Interfaces* **2020**, *12*, 36478–36484. [CrossRef] [PubMed]
42. Chen, J.; Xu, L.; Yang, M.; Chen, X.; Chen, X.; Hong, W. Highly stretchable photonic crystal hydrogels for a sensitive mechanochromic sensor and direct ink writing. *Chem. Mater.* **2019**, *31*, 8918–8926. [CrossRef]
43. Thorarinsdottir, A.E.; Harris, T.D. Metal–organic framework magnets. *Chem. Rev.* **2020**, *120*, 8716–8789. [CrossRef] [PubMed]
44. Xiong, T.; Zhang, Y.; Lee, W.S.V.; Xue, J. Defect engineering in manganese-based oxides for aqueous rechargeable zinc-ion batteries: A review. *Adv. Energy Mater.* **2020**, *10*, 2001769. [CrossRef]
45. Liu, H.; Li, J.; Zhang, X.; Liu, X.; Yan, Y.; Chen, F.; Zhang, G.; Duan, H. Ultrathin and ultralight Zn micromesh-induced spatial-selection deposition for flexible high-specific-energy Zn-ion batteries. *Adv. Funct. Mater.* **2021**, *31*, 2106550. [CrossRef]
46. Xu, X.; Chen, Y.; Liu, D.; Zheng, D.; Dai, X.; Shi, W.; Cao, X. Metal-Organic Framework-Based Materials for Aqueous Zinc-Ion Batteries: Energy Storage Mechanism and Function. *Chem. Rec.* **2022**, *22*, e202200079. [CrossRef]
47. Wang, L.; Zhu, Y.; Du, C.; Ma, X.; Cao, C. Advances and challenges in metal–organic framework derived porous materials for batteries and electrocatalysis. *J. Mater. Chem. A* **2020**, *8*, 24895–24919. [CrossRef]

48. Yuksel, R.; Buyukcakir, O.; Seong, W.K.; Ruoff, R.S. Metal-organic framework integrated anodes for aqueous zinc-ion batteries. *Adv. Energy Mater.* **2020**, *10*, 1904215. [CrossRef]
49. Sheng, Z.; Qi, P.; Lu, Y.; Liu, G.; Chen, M.; Gan, X.; Qin, Y.; Hao, K.; Tang, Y. Nitrogen-Doped Metallic $MoS_2$ Derived from a Metal–Organic Framework for Aqueous Rechargeable Zinc-Ion Batteries. *ACS Appl. Mater. Interfaces* **2021**, *13*, 34495–34506. [CrossRef]
50. Bai, X.-J.; Chen, D.; Li, L.-L.; Shao, L.; He, W.-X.; Chen, H.; Li, Y.-N.; Zhang, X.-M.; Zhang, L.-Y.; Wang, T.-Q. Fabrication of MOF thin films at miscible liquid–liquid interface by spray method. *ACS Appl. Mater. Interfaces* **2018**, *10*, 25960–25966. [CrossRef]
51. Zacher, D.; Schmid, R.; Woell, C.; Fischer, R.A. Surface chemistry of metal–organic frameworks at the liquid–solid interface. *Angew. Chem. Int. Ed.* **2011**, *50*, 176–199. [CrossRef] [PubMed]
52. Yang, J.; Feng, X.; Lu, G.; Li, Y.; Mao, C.; Wen, Z.; Yuan, W. NaCl as a solid solvent to assist the mechanochemical synthesis and post-synthesis of hierarchical porous MOFs with high I 2 vapour uptake. *Dalton Trans.* **2018**, *47*, 5065–5071. [CrossRef]
53. Wang, X.; Zhang, B.; Feng, J.; Wang, L.; Wu, B.; Zhang, J.; Ou, X.; Hou, F.; Liang, J. Cu-MOF-derived and porous Cu0. 26V2O5@ C composite cathode for aqueous zinc-ion batteries. *Sustain. Mater. Technol.* **2020**, *26*, e00236.
54. Shao, G.; Hanaor, D.A.; Shen, X.; Gurlo, A. Freeze casting: From low-dimensional building blocks to aligned porous structures—A review of novel materials, methods, and applications. *Adv. Mater.* **2020**, *32*, 1907176. [CrossRef] [PubMed]
55. Chen, Y.; Zhang, L.; Yang, Y.; Pang, B.; Xu, W.; Duan, G.; Jiang, S.; Zhang, K. Recent progress on nanocellulose aerogels: Preparation, modification, composite fabrication, applications. *Adv. Mater.* **2021**, *33*, 2005569. [CrossRef]
56. Joukhdar, H.; Seifert, A.; Jüngst, T.; Groll, J.; Lord, M.S.; Rnjak-Kovacina, J. Ice templating soft matter: Fundamental principles and fabrication approaches to tailor pore structure and morphology and their biomedical applications. *Adv. Mater.* **2021**, *33*, 2100091. [CrossRef]
57. Lei, C.; Xie, Z.; Wu, K.; Fu, Q. Controlled vertically aligned structures in polymer composites: Natural inspiration, structural processing, and functional application. *Adv. Mater.* **2021**, *33*, 2103495. [CrossRef]
58. Qiu, L.; Liu, J.Z.; Chang, S.L.; Wu, Y.; Li, D. Biomimetic superelastic graphene-based cellular monoliths. *Nat. Commun.* **2012**, *3*, 1241. [CrossRef]
59. Li, X.-H.; Liu, P.; Li, X.; An, F.; Min, P.; Liao, K.-N.; Yu, Z.-Z. Vertically aligned, ultralight and highly compressive all-graphitized graphene aerogels for highly thermally conductive polymer composites. *Carbon* **2018**, *140*, 624–633. [CrossRef]
60. Liu, D.; Lei, C.; Wu, K.; Fu, Q. A multidirectionally thermoconductive phase change material enables high and durable electricity via real-environment solar–thermal–electric conversion. *ACS Nano* **2020**, *14*, 15738–15747. [CrossRef]
61. Zhou, J.; Xie, M.; Wu, F.; Mei, Y.; Hao, Y.; Li, L.; Chen, R. Encapsulation of Metallic Zn in a Hybrid MXene/Graphene Aerogel as a Stable Zn Anode for Foldable Zn-Ion Batteries. *Adv. Mater.* **2022**, *34*, 2106897. [CrossRef] [PubMed]
62. Ling, W.; Yang, Q.; Mo, F.; Lei, H.; Wang, J.; Jiao, Y.; Qiu, Y.; Chen, T.; Huang, Y. An ultrahigh rate dendrite-free Zn metal deposition/striping enabled by silver nanowire aerogel with optimal atomic affinity with Zn. *Energy Storage Mater.* **2022**, *51*, 453–464. [CrossRef]
63. Kim, J.M.; Huh, Y.S.; Han, Y.-K.; Cho, M.S.; Kim, H.J. Facile synthesis route to highly crystalline mesoporous γ-$MnO_2$ nanospheres. *Electrochem. Commun.* **2012**, *14*, 32–35. [CrossRef]
64. Huang, R.; Liu, Y.; Chen, Z.; Pan, D.; Li, Z.; Wu, M.; Shek, C.-H.; Wu, C.L.; Lai, J.K. Fe-species-loaded mesoporous $MnO_2$ superstructural requirements for enhanced catalysis. *ACS Appl. Mater. Interfaces* **2015**, *7*, 3949–3959. [CrossRef] [PubMed]
65. Saroyan, H.S.; Bele, S.; Giannakoudakis, D.A.; Samanidou, V.F.; Bandosz, T.J.; Deliyanni, E.A. Degradation of endocrine disruptor, bisphenol-A, on an mixed oxidation state manganese oxide/modified graphite oxide composite: A role of carbonaceous phase. *J. Colloid Interface Sci.* **2019**, *539*, 516–524. [CrossRef]
66. Ha, H.-W.; Kim, T.W.; Choy, J.-H.; Hwang, S.-J. Relationship between electrode performance and chemical bonding nature in mesoporous metal oxide-layered titanate nanohybrids. *J. Phys. Chem. C* **2009**, *113*, 21941–21948. [CrossRef]
67. Kijima, N.; Sakao, M.; Manabe, T.; Akimoto, J. Electrochemical Properties of Titanium Oxides with Disordered Layer Stacking through Flocculation of Exfoliated Titania Nanosheets. *J. Electrochem. Soc.* **2019**, *166*, A5301. [CrossRef]
68. Ke, F.-S.; Huang, L.; Wei, H.-B.; Cai, J.-S.; Fan, X.-Y.; Yang, F.-Z.; Sun, S.-G. Fabrication and properties of macroporous tin–cobalt alloy film electrodes for lithium-ion batteries. *J. Power Sources* **2007**, *170*, 450–455. [CrossRef]
69. Liang, S.; Cheng, Y.J.; Zhu, J.; Xia, Y.; Müller-Buschbaum, P. A chronicle review of nonsilicon (Sn, Sb, Ge)-based lithium/sodium-ion battery alloying anodes. *Small Methods* **2020**, *4*, 2000218. [CrossRef]
70. Pang, Z.; Ding, B.; Wang, J.; Wang, Y.; Xu, L.; Zhou, L.; Jiang, X.; Yan, X.; Hill, J.P.; Yu, L. Metal-ion inserted vanadium oxide nanoribbons as high-performance cathodes for aqueous zinc-ion batteries. *Chem. Eng. J.* **2022**, *446*, 136861. [CrossRef]
71. Chen, L.; Yang, Z.; Cui, F.; Meng, J.; Chen, H.; Zeng, X. Enhanced rate and cycling performances of hollow $V_2O_5$ nanospheres for aqueous zinc ion battery cathode. *Appl. Surf. Sci.* **2020**, *507*, 145137. [CrossRef]
72. Li, R.; Zhang, H.; Zheng, Q.; Li, X. Porous V 2 O 5 yolk–shell microspheres for zinc ion battery cathodes: Activation responsible for enhanced capacity and rate performance. *J. Mater. Chem. A* **2020**, *8*, 5186–5193. [CrossRef]